Paleoclimate and current climate collectively shape the phylogenetic and functional diversity of trees worldwide

Wen-Yong Guo[1,2][*], Josep M. Serra-Diaz[3], Franziska Schrodt[4], Wolf L. Eiserhardt[2], Brian S. Maitner[5], Cory Merow[6], Cyrille Violle[7], Anne Blach-Overgaard[1,2], Jian Zhang[8], Madhur Anand[9], Michaël Belluau[10], Hans Henrik Bruun[11], Chaeho Byun[12], Jane A. Catford[13], Bruno E. L. Cerabolini[14], Eduardo Chacón-Madrigal[15], Daniela Ciccarelli[16], Johannes H. C. Cornelissen[17], Anh Tuan Dang-Le[18], Angel de Frutos[19], Arildo S. Dias[20], Aelton B. Giroldo[21], Alvaro G. Gutiérrez[22], Wesley Hattingh[23], Tianhua He[24,25], Peter Hietz[26], Nate Hough-Snee[27], Steven Jansen[28], Jens Kattge[19,29], Tamir Klein[30], Benjamin Komac[31], Nathan Kraft[32], Koen Kramer[33], Sandra Lavorel[34], Christopher H. Lusk[35], Adam R. Martin[36], Maurizio Mencuccini[37,38], Sean T. Michaletz[39], Vanessa Minden[40,41], Akira S. Mori[42], Ülo Niinemets[43], Yusuke Onoda[44], Renske E. Onstein[19], Josep Peñuelas[38,45], Valério D. Pillar[46], Jan Pisek[47], Matthew J. Pound[48], Bjorn J.M. Robroek[49], Brandon Schamp[50], Martijn Slot[51], Ênio Sosinski[52], Nadejda A. Soudzilovskaia[53], Nelson Thiffault[54], Peter van Bodegom[53], Fons van der Plas[55], Ian J. Wright[56], Jingming Zheng[57], Brian J. Enquist[5,58], Jens-Christian Svenning[1,2]

Affiliations

[1]Center for Biodiversity Dynamics in a Changing World (BIOCHANGE), Department of Biology, Aarhus University, 8000 Aarhus C, Denmark; wenyong.guo@bios.au.dk; guowyhgy@gmail.com (WYG); anne.overgaard@bios.au.dk (ABO); svenning@bios.au.dk (JCS)

[2]Section for Ecoinformatics & Biodiversity, Department of Biology, Aarhus University, 8000 Aarhus C, Denmark ; wolf.eiserhardt@bios.au.dk (WLE)

[3]Université de Lorraine, AgroParisTech, INRAE, Silva, Nancy, France; pep.serradiaz@agroparistech.fr

[4]School of Geography, University of Nottingham, Nottingham, NG7 2RD, United Kingdom; f.i.schrodt@gmail.com

[5]Department of Ecology and Evolutionary Biology, University of Arizona, Tucson AZ 85721, USA; bmaitner@gmail.com (BSM); brianjenquist@gmail.com (BJE)

[6]Ecology and Evolutionary Biology, University of Connecticut, Storrs, CT, USA; cory.merow@gmail.com

28 [7]UMR 5175 CEFE, Centre d'Ecologie Fonctionnelle et Evolutive, Univ Montpellier, CNRS, EPHE, IRD, Univ Paul
29   Valéry Montpellier 3, Montpellier, France; Cyrille.VIOLLE@cefe.cnrs.fr

30 [8]Zhejiang Tiantong Forest Ecosystem National Observation and Research Station, School of Ecological and
31   Environmental Sciences, East China Normal University, Shanghai, 200241, P.R. China;
32   jzhang@des.ecnu.edu.cn

33 [9]School of Environmental Sciences, University of Guelph, Guelph, Ontario, Canada; anand.madhur@gmail.com

34 [10]Centre for Forest Research, Département des sciences biologiques, Université du Québec à Montréal, PO Box 8888,
35   Centre-ville station, Montréal (Qc) H3C 3P8, Canada; michael.belluau@usherbrooke.ca

36 [11]Department of Biology, University of Copenhagen, 2100 Copenhagen Ø, Denmark; HHBruun@bio.ku.dk

37 [12]Department of Biological Sciences and Biotechnology, Andong National University, Andong, 36729, Korea;
38   chaehobyun@anu.ac.kr

39 [13]Department of Geography, King's College London, London, WC2B 4BG, UK; jane.catford@kcl.ac.uk

40 [14]Department of Biotechnology and Life Sciences, University of Insubria, Varese, Italy; bruno.cerabolini@uninsubria.it

41 [15]Escuela de Biología, Universidad de Costa Rica; 11501-2060 San Jose, Costa Rica; edchacon@gmail.com

42 [16]Department of Biology, University of Pisa, Via Luca Ghini 13, 56126 Pisa, Italy; daniela.ciccarelli@unipi.it

43 [17]Department of Ecological Science, Faculty of Science, Vrije Universiteit, 1081 HV Amsterdam, The Netherlands;
44   j.h.c.cornelissen@vu.nl

45 [18]University of Science, Ho Chi Minh City, Vietnam; Vietnam National University, Ho Chi Minh City, Vietnam;
46   dlatuan@gmail.com

47 [19]German Centre for Integrative Biodiversity Research (iDiv) Halle-Jena-Leipzig, Deutscher Platz 5e, 04103 Leipzig,
48   Germany; adefrutost@gmail.com (AdF); jkattge@bgc-jena.mpg.de (JK); onsteinre@gmail.com (REO);

49 [20]Goethe University, Institute for Physical Geography, Altenhöferallee 1, 60438 Frankfurt am Main, Germany;
50   arildodias@gmail.com

51 [21]Departamento de Ensino, Instituto Federal de Educação, Ciências e Tecnologia do Ceará - IFCE campus Crateús,
52   Avenida Geraldo Barbosa Marques, 567, Crateús, Brazil. 63708-260; aeltonbg@gmail.com

53 [22]Departamento de Ciencias Ambientales y Recursos Naturales Renovables, Facultad de Ciencias Agronómicas,
54   Universidad de Chile, Santa Rosa 11315, La Pintana, Santiago, Chile; bosqueciencia@gmail.com

55 [23]Global Systems and Analytics, Nova Pioneer, Paulshof, Gauteng, South Africa; wesnhattingh@gmail.com

56 [24]School of Molecular and Life Sciences, Curtin University, PO Box U1987, Perth, WA 6845, Australia;
57   Tianhua.He@curtin.edu.au

58 [25]College of Science, Health, Engineering and Education, Murdoch University, Murdoch, WA, Australia;

59 [26]Institute of Botany, University of Natural Resources and Life Sciences Vienna, Austria; peter.hietz@boku.ac.at

60 [27]Four Peaks Environmental Science and Data Solutions, Wenatchee, WA 98801 USA;
61   nhoughsnee@fourpeaksenv.com

62 [28]Institute of Systematic Botany and Ecology, Ulm University, 89081 Ulm, Germany; steven.jansen@uni-ulm.de

63 [29]Max Planck Institute for Biogeochemistry, Hans Knöll Str. 10, 07745 Jena, Germany;

64 [30]Department of Plant & Environmental Sciences, Weizmann Institute of Science, 76100 Rehovot, Israel;
65   tamir.klein@weizmann.ac.il

66   [31]Centre d'Estudis de la Neu i la Muntanya d'Andorra, Institut d'Estudis Andorrans (CENMA - IEA), Avinguda
67   Rocafort 21–23, AD600 Sant Julià de Lòria, Principality of Andorra; bkomac.cenma@iea.ad

68   [32]Department of Ecology and Evolutionary Biology, University of California, Los Angeles; Los Angeles, CA 90095,
69   USA; nkraft@ucla.edu

70   [33]Wageningen University, Forest Ecology and Management group, Droevendaalseseeeg 4 6700 AA Wageningen; and
71   Land Life Company, Mauritskade 63, 1092AD Amsterdam; koen.kramer@wur.nl

72   [34]Laboratoire d'Ecologie Alpine, LECA, UMR UGA-USMB-CNRS 5553, Université Grenoble Alpes, CS 40700,
73   38058 Grenoble Cedex 9, France; sandra.lavorel@univ-grenoble-alpes.fr

74   [35]Environmental Research Institute, University of Waikato, Hamilton, New Zealand; clusk@waikato.ac.nz

75   [36]Department of Physical and Environmental Sciences, University of Toronto Scarborough. 1265 Military Trail, M1C
76   1A4 Toronto, Ontario, Canada; adam.martin@utoronto.ca

77   [37]ICREA, Barcelona, Spain; m.mencuccini@creaf.uab.es

78   [38]CREAF, Cerdanyola del Vallès, Barcelona 08193, Catalonia, Spain; josep.penuelas@uab.cat

79   [39]Department of Botany and Biodiversity Research Centre, University of British Columbia, Vancouver, BC V6T 1Z4,
80   Canada; sean.michaletz@ubc.ca

81   [40]Department of Biology, Vrije Universiteit Brussel, Pleinlaan 2, 1050 Brussels, Belgium; vanessa.minden@uni-
82   oldenburg.de

83   [41]Institute for Biology and Environmental Sciences, University of Oldenburg, 26129 Oldenburg, Germany;

84   [42]Graduate School of Environment and Information Sciences, Yokohama National University, 79-7 Tokiwadai,
85   Hodogaya, Yokohama, 240-8501, Japan; akira.s.mori@gmail.com

86   [43]Estonian University of Life Sciences, Kreutzwaldi 1, 51006 Tartu, Estonia; ylo.niinemets@emu.ee

87   [44]Division of Forest and Biomaterials Science, Graduate School of Agriculture, Kyoto University, Oiwake,
88   Kitashirakawa, Kyoto, 606-8502 Japan; onoda@kais.kyoto-u.ac.jp; yusuke.onoda@gmail.com

89   [45]CSIC, Global Ecology Unit CREAF- CSIC-UAB, Bellaterra, Barcelona 08193, Catalonia, Spain;

90   [46]Department of Ecology, Universidade Federal do Rio Grande do Sul, Porto Alegre, 91501-970, Brazil;
91   vpillar@ufrgs.br

92   [47]Tartu Observatory, University of Tartu, Observatooriumi 1, Tõravere, 61602, Tartumaa, Estonia;
93   janpisek@gmail.com

94   [48]Department of Geography and Environmental Sciences, Northumbria University, Newcastle upon Tyne, NE1 8ST,
95   United Kingdom; matthew.pound@northumbria.ac.uk

96   [49]Aquatic Ecology & Environmental Biology Group, Faculty of Science, Institute for Water and Wetland Research,
97   Radboud University Nijmegen, Netherlands; Bjorn.Robroek@ru.nl

98   [50]Department of Biology, Algoma University, Sault Ste. Marie, Ontario, P6A 2G4, Canada;
99   Brandon.Schamp@algomau.ca

100   [51]Smithsonian Tropical Research Institute, Apartado 0843-03092, Balboa, Ancón, Republic of Panama; slotm@si.edu

101   [52]Embrapa Recursos Genéticos e Biotecnologia, 70770-917, Brasília, DF, Brazil; enio.sosinski@embrapa.br

102   [53]Institute of Environmental Sciences, Leiden University, 2333 CC Leiden, the Netherlands;
103   n.a.soudzilovskaia@cml.leidenuniv.nl (NS); p.m.van.bodegom@cml.leidenuniv.nl (PMvB)

104 [54]Natural Resources Canada, Canadian Wood Fibre Centre, 1055 du P.E.P.S., P.O. Box 10380, Stn. Sainte-Foy, Quebec,
105   QC G1V 4C7, Canada; nelson.thiffault@canada.ca

106 [55]Systematic Botany and Functional Biodiversity, Life science, Leipzig University, Germany;
107   fonsvanderplas@gmail.com

108 [56]Department of Biological Sciences, Macquarie University, North Ryde, NSW, 2109, Australia; ian.wright@mq.edu.au

109 [57]Beijing Key Laboratory for Forest Resources and Ecosystem Processes, Beijing Forestry University, Beijing, 100083,
110   P. R. China; zhjmbjfu@yahoo.com

111 [58]The Santa Fe Institute, 1399 Hyde Park Rd, Santa Fe, NM 87501, USA.

112 **ORCID**:

113 Wen-Yong Guo: https://orcid.org/0000-0002-4737-2042

114 Josep M. Serra-Diaz: https://orcid.org/0000-0003-1988-1154

115 Wolf L. Eiserhardt: https://orcid.org/0000-0002-8136-5233

116 Anne Blach-Overgaard: https://orcid.org/0000-0002-0200-1547

117 Jian Zhang: https://orcid.org/0000-0003-0589-6267

118 Hans Henrik Bruun https://orcid.org/0000-0003-0674-2577

119 Jane A. Catford: https://orcid.org/0000-0003-0582-5960

120 Bruno E. L. Cerabolini: https://orcid.org/0000-0002-3793-0733

121 Eduardo Chacón-Madrigal: https://orcid.org/0000-0002-8328-5456

122 Anh Tuan Dang-Le: https://orcid.org/0000-0002-9794-0669

123 Arildo S. Dias: https://orcid.org/0000-0002-5495-3435

124 Alvaro G. Gutiérrez: https://orcid.org/0000-0001-8928-3198

125 Wesley Hattingh: https://orcid.org/0000-0002-3626-5137

126 Nate Hough-Snee: https://orcid.org/0000-0003-4581-0931

127 Steven Jansen: https://orcid.org/0000-0002-4476-5334

128 Jens Kattge: https://orcid.org/0000-0002-1022-8469

129 Maurizio Mencuccini: http://orcid.org/0000-0003-0840-1477

130 Vanessa Minden: https://orcid.org/0000-0002-4933-5931

131   Akira S Mori: https://orcid.org/0000-0002-8422-1198

132   Ülo Niinemets: https://orcid.org/0000-0002-3078-2192

133   Josep Peñuelas: https://orcid.org/0000-0002-7215-0150

134   Jan Pisek: https://orcid.org/0000-0003-0396-2072

135   Matthew Pound: https://orcid.org/0000-0001-8029-9548

136   Bjorn JM Robroek: https://orcid.org/0000-0002-6714-0652

137   Martijn Slot: https://orcid.org/0000-0002-5558-1792

138   Nelson Thiffault: https://orcid.org/0000-0003-2017-6890

139   Ian J. Wright: https://orcid.org/0000-0001-8338-9143

140   Brian J. Enquist; https://orcid.org/0000-0002-6124-7096

141   Jens-Christian Svenning: https://orcid.org/0000-0002-3415-0862

Abstract

Trees are of vital importance for ecosystem functioning and services at local to global scales, yet we

still lack a detailed overview of the global patterns of tree diversity and the underlying drivers,

particularly the imprint of paleoclimate. Here, we present the high-resolution (110 km) worldwide

mapping of tree species richness, functional and phylogenetic diversities based on ~7 million

quality-assessed occurrences for 46,752 tree species (80.5% of the estimated total number of tree

species), and subsequent assessments of the influence of paleo−climate legacies on these patterns.

All three tree diversity dimensions exhibited the expected latitudinal decline. Contemporary

climate emerged as the strongest driver of all diversity patterns, with Pleistocene and deeper-time

($>10^7$ years) paleoclimate as important co-determinants, and, notably, with past cold and drought

stress being linked to reduced current diversity. These findings demonstrate that tree diversity is

affected by paleoclimate millions of years back in time and highlight the potential for tree diversity

losses from future climate change.

155 Understanding the global distribution of tree diversity and its underlying drivers has been an

156 enduring pursuit of scientists, at least as far back as Alexander von Humboldt. Achieving this aim is

157 becoming ever more urgent due to forest degradation and land use change [1–4], and also for aiding

158 forest restoration efforts [5]. Although our understanding of the global extent of tree cover has been

159 greatly improved via remote sensing [6] and large networks of forest tree plots [7,8], there are still gaps

160 in our knowledge of the global patterns and drivers of tree diversity. Previous studies have often

161 focused on tree species richness (SR) (e.g., [9]). However, SR does not directly represent species'

162 evolutionary history and does not provide trait-based insight into their functioning and role in

163 ecosystems. Phylogenetic diversity (PD; [10,11]) and functional diversity (FD; [12]) have been

164 introduced as promising, more informative biodiversity variables than SR and have been

165 successfully used in a wide variety of ecological applications, including conservation prioritization

166 [13–15]. Indeed, FD is better coupled than SR to ecosystem functioning, e.g., productivity responses to

167 climate change and forest multi-functionality [16–18]. In addition, PD and FD are more informative

168 than SR in describing mechanisms of species coexistence and ecosystem functioning [19,20], and thus

169 shed light on species extinction and conservation [13,14,21–23].

170 Many studies have emphasized the importance of current climate and edaphic conditions as key

171 determinants of species diversity (e.g., [24,25]). However, paleoclimate could leave an influential

172 legacy, e.g. via speciation, extinction or dispersal, on contemporary SR, and on phylogenetic and

173 functional structures of forest ecosystems [8,26–32]. Earth climate has experienced continuous changes

174 during geological time [33], such as cooling or warming trends and events, and major climatic

175 transitional periods have coincided with global ecosystem shifts [34–37]. Climatically-stable regions

176 tend to have high speciation and low extinction rates, resulting in higher SR, FD, and PD [38,39].

177 Contrastingly, wide climate oscillations (like glacial-interglacial cycles) can dramatically truncate

178 species' ranges and the chances of local diversification and adaptation, increasing the likelihood of

7

179   extinction and the removal of species with suboptimal traits, thereby decreasing all three facets of

180   diversity [40–43]. However, rapid climate change may alternatively cause range fragmentation and

181   further allopatric speciation as the result of isolation, potentially increasing net diversification rates

182   [27].

183   Due to the non-equivalency between the facets of diversity [44–47], the responses of SR, PD and FD to

184   different climatic conditions may vary. For example, warm and humid climates are hypothesized to

185   increase diversification rates [48,49], dispersal and establishment [50], and decrease extinction [27,51], thus

186   increasing SR and PD, but not necessarily FD, as comparable climates more likely predispose

187   species towards similar functional traits [25,52–55]. Thus, contemporary species diversity patterns can

188   be the result of historical climate legacies and present-day environment, although the relative

189   importance of these factors for FD and PD could be different.

190   Variable geological climates, i.e., warm and humid, or cold and dry in different paleo-time periods,

191   had remarkably divergent influences on tree diversities. However, previous studies have

192   concentrated mostly on assessing the effect of the cold and dry Last Glacial Maximum (LGM)

193   imprints that occurred ~27 – 19 thousand years ago (kya), but deeper-time perspectives may also be

194   important. For instance, ref. [26] found that palm tree diversity in Africa was affected by deep-time

195   climate during the late Pliocene (3.3 – 3.0 million years ago [mya]) and the late Miocene (11.6 – 7.3

196   mya), respectively. Similarly, ref. [27] found that the late Miocene climate influenced global patterns

197   of conifer phylogenetic structure. Recently, ref. [31] reported opposite effects of LGM and Miocene

198   tree cover on tree phylogenetic endemism. Hence, considering paleoclimate jointly across a range

199   of time frames could be helpful in better understanding the factors shaping tree diversities. However,

200   only a few SR studies have explicitly considered this [26], and even fewer in FD and PD research [42].

201   Here, we go beyond global mapping of tree species richness [9] by estimating species composition

202   and, based thereon, functional and phylogenetic diversity. We subsequently analyze the relative

203   roles of past and present climates in shaping global patterns of tree SR, FD, and PD. We first

204   compiled the most updated dataset of tree species including occurrence records, functional traits,

205   and tree phylogeny, covering 46,752 tree species or 80.5% of the species in the GlobalTreeSearch

206   list [47,56,57]. We subsequently mapped global tree SR, FD, and PD. To understand the potential

207   effects of paleoclimatic change on tree diversities completely, we examined the relative importance

208   of three paleoclimatic states in determining current SR, FD and PD patterns, with consideration of

209   other potential contemporary covariates, such as current climate, elevation, and human activities

210   (Table S1). Specifically, we explored the influence of paleoclimate related to important climate

211   states of the late Cenozoic, the time frame where current species diversity to a large extent have

212   evolved: i) the warm and humid late Miocene, *ca*. 11.63 – 7.25 mya; the mid-Pliocene Warm period,

213   *ca*. 3.264 – 3.025 mya; the cold and dry Pleistocene glaciations (represented by the LGM, ~ 21 kya);

214   and Pleistocene warm interglacials (IG, ~ 787 kya and ~ 130 kya) (Figs. S1 & S2). In doing so, our

215   study addressed three main goals: (1) mapping global contemporary tree SR, FD and PD; (2)

216   assessing the relative importance of present-day environment, Quaternary glacial-interglacial

217   oscillations, and deeper-time effects on today's SR, FD and PD patterns, to help understand the

218   fundamental processes determining accumulation and maintenance of tree diversity; and (3)

219   investigating spatial divergence between FD and PD, and identifying the underlying driving factors.

Results

Global patterns of tree diversities

222   The global tree SR, FD, and PD distributions show classic latitudinal gradients [58–60], with low

223   diversities at high latitudes and the highest diversities in the tropics (grid cell maximum value of

224 3261 spp. for SR and cumulative branch lengths of 641 and 61,183 Myrs for FD and PD,

225 respectively at 110 km resolution, Fig. S3), particularly in the Neotropical lowlands (Amazonia)

226 (Fig. 1). The latitudinal pattern is stronger in America and Asia-Australasia than in Africa-Europe,

227 due to the interruption of the diversity gradients by deserts in northern Africa, where the diversity

228 indices (SR, FD, and PD) are as low as at latitudes harboring the boreal climate. The similarity of

229 the spatial patterns among the three diversity measures reflects the monotonic relationships

230 observed between them (Fig. S4).

231 **Drivers of global tree diversity**

232 Due to the high associations between SR, FD, and PD, their individual relationships with the tested

233 predictors are mostly consistent (Figs. 2 & Table S2). After controlling for spatial autocorrelation,

234 simultaneous autoregressive models (SARs) explain more than 94% (global models) and 78%

235 (regional models) of the variance (Table S2) in the response variables (SR, PD, and FD). Present-

236 day annual precipitation (AP) and mean annual temperature (MAT) are the overall strongest drivers

237 with positive effects on SR, FD, and PD globally, and for AP also regionally except for two regions

238 where other drivers are stronger (Australasia, Nearctic). The effect of MAT varies in strength and

239 sign among regions, showing both positive and negative effects on diversity (Fig. 2, Table S2).

240 Elevation range and human modification index (HMc) have consistent positive effects on SR, FD

241 and PD globally as well as regionally. Four out of the six paleoclimatic variables show significant

242 relations to all three diversity dimensions (Fig. 2). Globally, the Miocene MAT anomaly (i.e.,

243 Miocene MAT minus present MAT), the Miocene AP anomaly, and the LGM AP anomaly have

244 positive relations to all diversity indices, while the LGM MAT anomaly have a weak negative

245 relation to SR ($p < 0.05$, Table S2) and no relation to FD and PD (Fig. 2). Hence, SR, PD and FD

246 consistently increase with increasing high precipitation in the Miocene and LGM relative to the

247   present, while SR, but not FD or PD, is generally reduced by increasing warm during LGM at a

248   global scale. However, although some of these global relationships are mirrored regionally, not all

249   paleoclimatic predictors are significant nor show consistent relationships across the biogeographic

250   regions, e.g., with LGM AP anomaly showing negative associations in Australasia and Miocene

251   MAT anomaly in Afrotropic for all three indices (Table S2).

252   Taken all together, precipitation-related effects were stronger and more consistent (among regions)

253   climatic drivers of diversity (SR, FD, PD) than were temperature-related effects, with this true both

254   for current climate (AP) and for paleoclimates (Miocene AP anomaly; IG AP anomaly).

Spatial divergence between functional and phylogenetic diversities and its drivers

256   FD and PD are tightly and positively related (Fig. S4c). Deviations (FD residuals) from this linear

257   relationship show marked spatial patterning (Fig. 3). Across North America, western and southern

258   Europe, central Africa, eastern Asia, and eastern Australia, FD is generally higher than predicted by

259   PD (i.e., overdispersion), whilst the opposite (i.e., FD deficit) is revealed in western Australia, much

260   of southern and eastern Africa, west of the Andes (Peru), and central parts of northern Eurasia.

261   The relative importance of the factors explaining variation in FD residuals are different from those

262   explaining their variations (Fig. 4 vs. Fig. 2b & 2c). Overall, current AP is correlated negatively

263   with the FD residuals both globally and regionally, but is only the strongest driver at global scale

264   (Figs. 4 & 5, Table S3). MAT and non-climatic factors show weak or no relations, except for MAT

265   for Indo-Maley and the Neotropics. The effects of the paleoclimate are variable. At global scale, the

266   Miocene AP anomaly and the LGM MAT anomaly are negatively related to the FD residuals, while

267   the LGM AP anomaly is positively related (Figs. 4 & 5). However, these relationships are

268   inconsistent across biogeographic regions (Figs. 4 & 5).

Discussion

Based on an unprecedented tree occurrence database, our study maps strong latitudinal patterns in all three diversity dimensions (SR, PD, and FD) at global scale. The SR-linked global latitudinal patterns of Faith's PD and FD matches previous empirical and modeled studies of tree species richness (e.g., [9,61]), tree functional diversity in the New World [62], and tree phylogenetic diversity at a regional scale [31]. It has been reported that speciation in rainforest environments has taken place at least since the Paleocene (~58 mya) [63,64], probably coupled to jointly high temperatures and precipitation [38,49,51,65]. Moreover, the relatively stable environment, compared to high latitudes, may also resulted in low extinction rates, making the tropics both "cradles (species diversifying)" and "museums (species persistence)" of species diversity [49,66]. In addition, long speciation history and lower extinction rates in the tropics could result in both higher phylogenetic diversity and functional diversity [38,48,49,51, but see 35].

Our results provide evidence that paleoclimate complements current climate in shaping tree diversity globally and regionally, and that these effects are not only related to the recent prehistory – such as the Last Glacial period, represented by the LGM 21,000 years ago – but also much deeper time scales. These results extend previous findings for other organism groups notably for species richness and endemics [39,42] and for trees or plant clades including trees in specific regions and biomes [26,27,29,67–70], to trees globally. Importantly, they go beyond species richness to the more ecologically meaningful indices, functional and phylogenetic diversity.

Notably, we found that precipitation effects were stronger and more consistent (across regions) drivers than temperature effects, especially in relation to the wet and warm middle Miocene (11.6 – 7.5 mya), and the dry, cold LGM. The middle Miocene, the warmest and wettest interval in the late

12

291   Cenozoic, was a period of forest expansion [34,71], due to warming coupled with elevated atmospheric

292   CO_2 (>500 ppm) [72–74]. This likely promoted high species diversity globally due to a higher

293   diversification rate and lower extinction rate [38,48,51]. The Myrtaceae family [75] and the genus *Quercus*

294   [76] are examples that follow this pattern. As a legacy of forest expansion, the generally warmer and

295   wetter climate in the late Miocene compared to the contemporary climate have a positive

296   associations to tree SR, FD, and PD [37]. We also see this in our results at the global scale and for

297   most regions with positive effects of both Miocene AP and MAT (Fig. 2). The weak negative

298   association between the LGM MAT anomaly and SR, but not with FD and PD, could indicate that

299   global cold climate in LGM (Fig. S1) caused range extractions or even extinctions of certain species.

300   Likely, the intensity of these processes were not strong enough to significantly decrease the

301   communities' FD and PD, probably due to the high tree diversity accumulated in previous warm

302   and humid periods [36,75]. Indeed, both tree FD and PD showed the tendency to level-off with SR

303   increase (Fig. S6), a similar pattern reported by [54], indicating that closely related tree species have

304   more similar traits, i.e., the functional space tightly packed [30,70]. The LGM precipitation anomaly

305   was positively related to tree SR, PD and FD, likely reflecting widespread forest contractions during

306   the generally dry LGM and tree survival in moist refugia [77,78]. Furthermore, the diversity of drier

307   forests itself is generally lower due to a limited number of niches and the physiological limits of

308   species drought tolerance [79]. Our results suggest that paleoclimate affects not just forest biodiversity,

309   but also forest ecosystem functioning given the effects found here, which corroborates other studies

310   on FD [16,17] and PD [20,27,67]. Notably, a recent study has found that paleoclimatic legacies in tree FD

311   negatively affect stand productivity in Northern Hemisphere temperate forests [80].

312   The relationships between paleoclimate and SR, FD, and PD were partially repeated within

313   biogeographic regions, there was also substantial inter-region variation in these relations (Fig. 2).

314   For example, not all of the four significant relationships found globally were retained regionally,

315   and new relations emerged in some cases. These variable regional relations may reflect differing

316   regional paleoclimatic histories, differences in the overall climatic and geographic setting, as well

317   as methodological effects, e.g., different covariation among explanatory variables. For example, in

318   Australasia, only the LGM AP anomaly showed significant, negative relationships with FD and PD,

319   possibly because the temperature there was rather stably high during the last millions of years, with

320   precipitation being more variable and lower (Fig. S2).

321   The regions representing FD surplus relative to PD, i.e., where species were found to be more

322   functionally diverse (high FD) than expected from PD, largely coincided with high SR regions (Figs.

323   3 & 1a), represented by warm and humid climate today. This suggests that communities in warm

324   and humid conditions have accumulated more FD than expected compared to dry or cold regions.

325   This FD surplus could be caused by high competition, high heterogeneous environments, or

326   otherwise diversifying trait evolution [19,62,81–83]. We found that all precipitation variables were

327   important for explaining the FD deviation from PD, even though their effects differed (Figs. 4 & 5).

328   Surprisingly, high current precipitation tended to correspond to FD deficits, i.e., areas where species

329   were more functionally similar than predicted by PD, both globally and in several biogeographic

330   regions. Even though the observed FD in many wet and warm areas were higher than expected from

331   PD, an explanation for the observed relationship could be that moist tropical forests harbor large

332   numbers of shade-tolerant species, which have evolved along a similar evolutionary path (i.e.,

333   stabilizing selection) to adapt to the shady environment, thus showing high levels of ecological

334   equivalence [83,84].

335   Building on recent progress in the harmonization of several databases on tree species distributions,

336   functional traits, phylogenetic relatedness, and global paleoclimate, we have found that the tropics

337   harbor the highest diversity across not only taxonomic, but also functional and phylogenetic

14

338   dimensions, while high latitudes have lower diversity values for all diversity measures.

339   Nevertheless, there are important and informative deviations between the patterns in FD and PD,

340   including a signature consistent with less ecological filtering in moist, shady tropical forest

341   environments [84]. Importantly, we found evidence that current tree phylogenetic and functional

342   diversities are likely shaped not only by the contemporary environment, but also by past climate as

343   far back as the Miocene (~10 Mya). Notably, we see long-term reductions in FD and PD in relation

344   to past climatic cold or drought stress, likely affecting current forest ecosystem functioning [80].

345   These findings highlight the importance of climate for tree diversity and forest ecosystems, and that

346   losses from future climate change could have strong and very long-lasting effects.

Methods

Tree species and their range maps

In this study, we used the world tree species list [56] and species range maps compiled by [47,57]. Briefly, the world tree species checklist (GlobalTreeSearch, GTS [56]) was used to extract the global tree species list for the current study. Tree species included in the GTS is based on the definition by the IUCN's Global Tree Specialist Group (GTSG), i.e., "a woody plant with usually a single stem growing to a height of at least two meters, or if multi-stemmed, then at least one vertical stem five centimeters in diameter at breast height" [56]. This list was subsequently standardized via the Taxonomic Name Resolution Service (TNRS) online tool [85] to remove synonyms. The occurrence records of the selected species were collated from five widely used and publicly accessible databases, namely: the Global Biodiversity Information Facility (GBIF; http://www.gbif.org), the public domain Botanical Information and Ecological Network v.3 (BIEN; http://bien.nceas.ucsb.edu/bien/;[86,87]), the Latin American Seasonally Dry Tropical Forest Floristic Network (DRYFLOR; http://www.dryflor.info/; [88]), the RAINBIO database (http://rainbio.cesab.org/; [89]), and the Atlas of Living Australia (ALA; http://www.ala.org.au/). The compiled occurrence data was accessed [57] and the high-quality records were then used to generate range maps based on the alpha hull algorithm via the *Alphahull* package [90,91] in R (ver. 3.5.1; [92]). We further validated the range maps using an external independent dataset [9]. The estimated range maps of the 46,752 tree species were rasterized to 110 km equal-area grid cells (~1 degree at the Equator), a resolution commonly used in global diversity studies (e.g.,[45]), using the *letsR* package [93]. For detailed information on the range map estimations and external validation, see [47].

Phylogeny

369   We constructed a phylogenetic tree for the tree species using the largest seed-plant phylogeny

370   presently available (the ALLMB tree [94]). This dated phylogeny combines a backbone tree [95], which

371   was built using sequence data from public repositories (GenBank) to reflect deep relationships, with

372   previous knowledge of phylogenetic relationships and species names from the Open Tree of Life

373   (Open Tree of Life synthetic tree release 9.1 and taxonomy version 3,

374   https://tree.opentreeoflife.org/about/synthesis-release/v9.1). This phylogeny was matched to our

375   tree species dataset, and any species that were not in our dataset were removed from the tree.

376   Subsequently, some species missing from the phylogeny were manually added, using the same

377   approach as ref. [94].

Functional trait data

379   Eight ecologically relevant and commonly used traits [96] were selected for functional diversity

380   analyses, i.e., leaf nitrogen content, wood density, leaf phosphorus content, leaf dry matter content,

381   plant max height, seed dry mass, specific leaf area, and leaf area. Originally, we compiled 21

382   functional traits from the TRY (https://try-db.org/TryWeb/Home.php; [97,98], TOPIC [99–105], and BIEN

383   (http://bien.nceas.ucsb.edu/bien/; [86,87]) databases. As many of the species' trait were missing, we

384   imputed missing values via an gap-filling algorithm with Bayesian Hierarchical Probabilistic Matrix

385   Factorization (BHPMF, [106–108]), which is mostly based on both trait-trait correlation matrix and the

386   phylogentic signal of traits (Refer to ref. [47] for the detailed gap-filling procedure). In this process,

387   all the 21 traits were used to maximally benefit from the correlations among them.

Environmental variables

389   We compiled 17 environmental variables, including current climate, paleo-climate, human effects,

390   topographic heterogeneity and evolutionary history (Supplementary Table S1). Climate, both

391   present-day and paleoclimate, is generally assumed to be a vital predictor of species distribution and

392   diversity patterns (e.g., [26,27,29,39,109,110]). Due to the data availability of the paleoclimates, we

393   included two bioclimatic predictors commonly used in relevant studies: annual mean temperature

394   (MAT) and annual precipitation (AP). Current climate variables were extracted from WorldClim

395   (v.2, www.worldclim.org) at a resolution of 30 arc-seconds (~1 km at the equator), averaging global

396   climate data from the period 1970 - 2000 [111]. We selected six paleo-time periods spanning from *ca.*

397   11.6 – 7.2 mya to *ca.* 21 kya, representing climatic conditions either warmer, cooler, or similar

398   compared to the present-day climate. Specifically, each bioclimatic layer of the late Miocene

399   climate (11.61 – 7.25 mya [37]) and mid-Pliocene Warm period (~ 3.264 – 3.025 mya; [112,113]) were

400   averaged to represent the warmer climate compared to present day (hereafter Miocene). Pliocene

401   Marine Isotope Stage M2, a glacial interval in the late Pliocene (~ 3.3 mya; [113,114]), was used to

402   represent the Pliocene global cooling period, while the Last Glacial Maximum (LGM, ~ 21 kya)

403   was used to present the more recent global cooling event compared to M2 [113,115]. We further

404   constructed a current climate (hereafter Interglacial, IG) analog using the mean value per

405   bioclimatic layer between the Pleistocene Marine Isotope Stage 19 (MIS 19), the oldest Pleistocene

406   interglacial (~ 787 kya [113]), and the Last Interglacial (LIG; ~ 130 kya [116]). The mid-Pliocene Warm

407   Period, Pliocene M2, Pleistocene MIS19, and the LIG data were extracted from Paleoclim

408   (www.paleoclim.org), at a resolution of 2.5 arc-minutes (~ 4.5 km at the equator) [113], and the LGM

409   data was extracted from the CHELSA database (www.chelsa-climate.org) at a resolution of 30 secs

410   [115].

411   In addition to climate, other factors, such as human activities, topographic heterogeneity, and

412   evolutionary history, can also affect plant distributions [9,26,117,118]. The Human Modification map

413   (HMc [119])[119] was used as a proxy of human activities. Compared to the commonly used human

414   footprint index and human influence index maps [120], HMc has been modelled with the incorporation

415   of 13 most recent global-scale anthropogenic layers (with the median year of 2016) to account for

416 the spatial extent, intensity, and co-occurrence of human activities, many of which showing high

417 direct or indirect impact on biodiversity [121]. HMc was extracted at a resolution of 1 km^2 [119]. The

418 elevation range is the absolute difference between the maximum and minimum elevation value

419 within a specific area. We computed the elevation/topographic range within each 110 ×110 km grid

420 cell based on the digital elevation model at 90 m resolution (http://srtm.csi.cgiar.org/). Elevation

421 range is a proxy of environmental heterogeneity, which is considered as a universal driver of

422 biological diversity [122,123]. To analyze the potential effects of evolutionary and biogeographic

423 history, we also included the biogeographic regions as an additional variable. We applied the

424 definition of biogeographic regions from ref. [124], which defines 12 regions globally using cladistic

425 and phylogenetic analyses of plant species, and plate tectonics. However, due to the varying data

426 size in each of the 12 regions, we combined them into six regions, i.e., Afrotropic, Australasia,

427 Indo-Malay, Nearctic, Neotropic, Palearctic, largely similar to the biogeographic realms proposed

428 by ref. [125]. All predictors were extracted from various databases, which we describe in further detail

429 in the supplement (Supplementary Table S1).

430 Except for the biogeographic regions and elevation range, mean values for all predictors were

431 extracted at a 110 ×110 km resolution. The variable extractions and averaging were carried out in

432 the *letsR* package. Due to the low reliability and/or missing environmental variables for many

433 islands [126], we removed insular grid cells from small islands, and 11,950 grid cells with records

434 were kept (Fig. S5).

Phylogenetic and functional diversity

436 Phylogenetic diversity (PD) was calculated for each 110 ×110 km grid cell as the sum of the branch

437 lengths of all co-occurring species as defined by ref. [10]. Among the many existing, somewhat

438   overlapping matrices of PD, the one we selected is the most widely used due to its easy calculation

439   and interpretation and a more robust basis for conservation [10,13,14].

440   Functional diversity (FD) was calculated in an analogous manner to PD [127]. A Principal Component

441   Analysis (PCA) was applied to the eight traits to eliminate trait redundancy. Values of all traits

442   were log transformed to improve normality and were standardized before analysis. Then a

443   dendrogram based on the first three PCs (explaining 84% of the total variation) was constructed

444   using Gower's distance via the *vegan* [128] and *fastcluster* [129] packages. This dendrogram was used to

445   calculate FD as the sum of the total branch lengths connecting a set of species in the 110 ×110 km

446   grid cell. Both PD and FD were calculated using the *letsR* and *picante* [130] packages.

447   To investigate the bivariate relationships between FD and PD, an ordinary least squares model was

448   implemented. We further plotted the residuals of model to show any deviation between FD and PD.

449   ### *Statistical analyses*

450   To test the long-term climate stability hypothesis, we calculated the anomaly for MAT and AP

451   between the four paleo-time periods and the present-day, i.e., past minus present, to represent the

452   amplitude of the climate changes within each time-scale (Fig. S1) [26,27,29,39,118]. On average,

453   compared to the present, mean annual temperature (MAT) was much higher in the Miocene, slightly

454   higher in the Pliocene M2 period, much lower in the LGM, and similar in the IG (Fig. S2a). During

455   Pliocene M2 and IG, annual precipitation (AP) was similar to the present-day, while the Miocene

456   and LGM had slightly higher or lower precipitation, respectively than the contemporary

457   precipitation (Fig. S2b). The paleo-time periods selected, thus, represent (on average) cold, warm,

458   and similar paleo-climates compared to present-day conditions.

459   Pearson correlation coefficients showed a low level of correlations between MAT, AP, and their

460   respective anomaly variables (Fig. S6). However, MAT and AP of Pliocene M2 and Pleistocene IG

461 anomaly showed relatively high correlations (Fig. S7) with or without accounting for the spatial

462 autocorrelation (using the *SpatialPack* package [131]). Consequently, we removed the two Pliocene

463 M2 variables from further analyses.

464 We used ordinary least squares models (OLSs) and simultaneous autoregressive models (SARs), if

465 the OLS model residuals exhibited spatial autocorrelation (SAC), to evaluate the relative

466 importance of the predictor variables in determining the variation in each of the three diversity

467 indices and the residuals of bivariate relationships between FD and PD. We used the SAR error

468 model because of its superior performance compared to other SAR model types [132]. The SAR error

469 model adds a spatial weights matrix to an OLS regression to accounts for SAC in the model

470 residuals. A series of spatial weights, i.e., k-means neighbor of each site, were tested and $k = 1.5$

471 was used for all SARs models as it can successfully account for the SAC (see Supplementary results

472 of statistical analyses). Residual SAC was examined in all models (both OLS and SAR) using

473 Moran's I test, and Moran's I correlograms were also used to visualize the spatial residuals of the

474 models. Model explanatory power was represented by adjusted R^2 (OLSs) and Nagelkerke pseudo-

475 R^2 (SARs) [133], while the Akaike Information Criterion (AIC) and Bayesian information criterion

476 (BIC) were used to compare the models for each diversity index [134]. SARs and Moran's I tests were

477 carried out using the *spdep* package [135]. Both OLS and SAR models were run by including current

478 MAT and AP, the six anomaly variables, and the other non-climate predictors (elevation range and

479 HMc) to investigate their relative contributions to each diversity index. In addition to the global

480 models, we ran the same models for each biogeographic region to test whether the global

481 relationships varied among regions. Moreover, we ran three additional global models for the FD and

482 PD indices, selecting only one paleoclimate (both MAT and AP) from the three paleo-time periods

483 at the time, and keeping other variables the same in each model to investigate whether the effects of

484 the different paleoclimate predictors changed compared to the full models (including all paleo

485 climatic predictors). Before running the models, we inspected the normality of all predictors and

486 $\log_{10}$-transformed variables if needed. All response variables (three diversity indices) were $\log_{10}$-

487 transformed. Thereafter, we standardized all predictor variables by transforming all variables to a

488 mean of zero and a standard deviation of one to derive more comparable estimates [136].

Supplementary results of statistical analyses

490 We found that for all models (both global and regional), SAR models performed better than the

491 corresponding OLS models, regarding to AIC, BIC, and R^2 (Tables S2-S3), and all SAR models

492 successfully accounted for SAC in model residuals ($p \gg 0.05$, Figs. S8-S11). Thus, we only

493 represented the results from SARs models in the text, even though the significance of some

494 predictors varied between OLS and SAR models (Fig. S12). In addition, we found that the effects of

495 paleoclimate variables showed no change between the full models, including all paleoclimate

496 variables and models using paleoclimate of each paleo-period (Fig. S13-S14). This clearly shows

497 the robustness of their relationships with the tree diversity indices.

22

498   **References**

499   1.   Chazdon, R. L. Beyond deforestation: Restoring forests and ecosystem services on degraded lands.
500   *Science* **320**, 1458–1460 (2008).

501   2.   Potapov, P. *et al.* The last frontiers of wilderness: Tracking loss of intact forest landscapes from 2000
502   to 2013. *Sci. Adv.* **3**, e1600821 (2017).

503   3.   Watson, J. E. M. *et al.* The exceptional value of intact forest ecosystems. *Nature Ecology and*
504   *Evolution* **2**, 599–610 (2018).

505   4.   Hansen, M. C., Stehman, S. V & Potapov, P. V. Quantification of global gross forest cover loss. *Proc.*
506   *Natl. Acad. Sci. U. S. A.* **107**, 8650–8655 (2010).

507   5.   Bastin, J. F. *et al.* The global tree restoration potential. *Science (80-.).* **364**, 76–79 (2019).

508   6.   Hansen, M. C. *et al.* High-resolution global maps of 21st-century forest cover change. *Science (80-.).*
509   **342**, 850–853 (2013).

510   7.   Crowther, T. W. *et al.* Mapping tree density at a global scale. *Nature* **525**, 201–205 (2015).

511   8.   Bruelheide, H. *et al.* Global trait–environment relationships of plant communities. *Nat. Ecol. Evol.* **2**,
512   1906–1917 (2018).

513   9.   Keil, P. & Chase, J. M. Global patterns and drivers of tree diversity integrated across a continuum of
514   spatial grains. *Nat. Ecol. Evol.* **3**, 390–399 (2019).

515   10.   Faith, D. P. Conservation evaluation and phylogenetic diversity. *Biol. Conserv.* **61**, 1–10 (1992).

516   11.   Faith, D. P. The PD Phylogenetic Diversity Framework: Linking Evolutionary History to Feature
517   Diversity for Biodiversity Conservation. in 39–56 (2016). doi:10.1007/978-3-319-22461-9_3

518   12.   Petchey, O. L. & Gaston, K. J. Functional diversity: Back to basics and looking forward. *Ecology*
519   *Letters* **9**, 741–758 (2006).

520   13.   Mazel, F. *et al.* Prioritizing phylogenetic diversity captures functional diversity unreliably. *Nat.*
521   *Commun.* **9**, 2888 (2018).

522   14.   Tucker, C. M. *et al.* A guide to phylogenetic metrics for conservation, community ecology and
523   macroecology. *Biol. Rev.* **92**, 698–715 (2017).

524   15.   Jarzyna, M. A. & Jetz, W. Detecting the Multiple Facets of Biodiversity. *Trends in Ecology and*
525   *Evolution* **31**, 527–538 (2016).

526   16.   Huang, X., Su, J., Li, S., Liu, W. & Lang, X. Functional diversity drives ecosystem multifunctionality in a
527   Pinus yunnanensis natural secondary forest. *Sci. Rep.* **9**, 1–8 (2019).

528   17.   Díaz, S. *et al.* Functional Diversity — at the Crossroads between Ecosystem Functioning and
529   Environmental Filters. in *Terrestrial Ecosystems in a Changing World* 81–91 (Springer, Berlin,
530   Heidelberg, 2007). doi:10.1007/978-3-540-32730-1_7

531   18.   Díaz, S. & Cabido, M. Vive la différence: Plant functional diversity matters to ecosystem processes.
532   *Trends in Ecology and Evolution* **16**, 646–655 (2001).

533   19.   Safi, K. *et al.* Understanding global patterns of mammalian functional and phylogenetic diversity.
534   *Philos. Trans. R. Soc. B Biol. Sci.* **366**, 2536–2544 (2011).

535　20.　Donoghue, M. J. A phylogenetic perspective on the distribution of plant diversity. *Proc. Natl. Acad.*
536　　　*Sci. U. S. A.* **105**, 11549–11555 (2008).

537　21.　Oliveira, B. F., Sheffers, B. R. & Costa, G. C. Decoupled erosion of amphibians' phylogenetic and
538　　　functional diversity due to extinction. *Glob. Ecol. Biogeogr.* **29**, 309–319 (2020).

539　22.　Faith, D. P. Phylogenetic diversity, functional trait diversity and extinction: Avoiding tipping points
540　　　and worst-case losses. *Philos. Trans. R. Soc. B Biol. Sci.* **370**, 1–10 (2015).

541　23.　Park, D. S., Feng, X. & Maitner, B. S. Darwin's naturalization conundrum can be explained by spatial
542　　　scale. *Proceedings of the National Academy of Sciences* 201918100 (2020).
543　　　doi:10.5281/zenodo.3710499

544　24.　Whittaker, R. J. & Field, R. Tree Species Richness Modelling: An Approach of Global Applicability?
545　　　*Oikos* **89**, 399–402 (2000).

546　25.　Wright, I. J. *et al.* Modulation of leaf economic traits and trait relationships by climate. *Glob. Ecol.*
547　　　*Biogeogr.* **14**, 411–421 (2005).

548　26.　Blach-Overgaard, A., Kissling, W. D., Dransfield, J., Balslev, H. & Svenning, J. C. Multimillion-year
549　　　climatic effects on palm species diversity in Africa. *Ecology* **94**, 2426–2435 (2013).

550　27.　Eiserhardt, W. L., Borchsenius, F., Sandel, B., Kissling, W. D. & Svenning, J. C. Late Cenozoic climate
551　　　and the phylogenetic structure of regional conifer floras world-wide. *Glob. Ecol. Biogeogr.* **24**, 1136–
552　　　1148 (2015).

553　28.　Ordonez, A. & Svenning, J.-C. Consistent role of Quaternary climate change in shaping current plant
554　　　functional diversity patterns across European plant orders. *Sci. Rep.* **7**, 42988 (2017).

555　29.　Svenning, J. C. & Skov, F. Could the tree diversity pattern in Europe be generated by postglacial
556　　　dispersal limitation? *Ecology Letters* **10**, 453–460 (2007).

557　30.　Ordonez, A. & Svenning, J. C. Geographic patterns in functional diversity deficits are linked to glacial-
558　　　interglacial climate stability and accessibility. *Glob. Ecol. Biogeogr.* **24**, 826–837 (2015).

559　31.　Sandel, B. *et al.* Current climate, isolation and history drive global patterns of tree phylogenetic
560　　　endemism. *Glob. Ecol. Biogeogr.* **29**, 4–15 (2020).

561　32.　Blonder, B. *et al.* Late Quaternary climate legacies in contemporary plant functional composition.
562　　　*Glob. Chang. Biol.* **24**, 4827–4840 (2018).

563　33.　Zachos, J., Pagani, H., Sloan, L., Thomas, E. & Billups, K. Trends, rhythms, and aberrations in global
564　　　climate 65 Ma to present. *Science* **292**, 686–693 (2001).

565　34.　Dunn, R. E., Strömberg, C. A. E., Madden, R. H., Kohn, M. J. & Carlini, A. A. Linked canopy, climate,
566　　　and faunal change in the Cenozoic of Patagonia. *Science (80-.).* **347**, 258–261 (2015).

567　35.　Meseguer, A. S. & Condamine, F. L. Ancient tropical extinctions at high latitudes contributed to the
568　　　latitudinal diversity gradient. *Evolution (N. Y).* evo.13967 (2020). doi:10.1111/evo.13967

569　36.　Herbert, T. D. *et al.* Late Miocene global cooling and the rise of modern ecosystems. *Nat. Geosci.* **9**,
570　　　843–847 (2016).

571　37.　Pound, M. J. *et al.* A Tortonian (Late Miocene, 11.61-7.25Ma) global vegetation reconstruction.
572　　　*Palaeogeogr. Palaeoclimatol. Palaeoecol.* **300**, 29–45 (2011).

573　38.　Svenning, J. C., Borchsenius, F., Bjorholm, S. & Balslev, H. High tropical net diversification drives the

574   New World latitudinal gradient in palm (Arecaceae) species richness. in *Journal of Biogeography* **35**,
575   394–406 (John Wiley & Sons, Ltd (10.1111), 2008).

576   39.   Sandel, B. *et al.* The influence of late quaternary climate-change velocity on species endemism.
577   *Science (80-.).* **334**, 660–664 (2011).

578   40.   McGlone, M. S., Buitenwerf, R. & Richardson, S. J. The formation of the oceanic temperate forests of
579   New Zealand. *New Zealand Journal of Botany* **54**, 128–155 (2016).

580   41.   Liebergesell, M. *et al.* Functional resilience against climate-driven extinctions - Comparing the
581   functional diversity of European and north American tree floras. *PLoS One* **11**, e0148607 (2016).

582   42.   Svenning, J.-C., Eiserhardt, W. L., Normand, S., Ordonez, A. & Sandel, B. The Influence of
583   Paleoclimate on Present-Day Patterns in Biodiversity and Ecosystems. *Annu. Rev. Ecol. Evol. Syst.* **46**,
584   551–572 (2015).

585   43.   Dynesius, M. & Jansson, R. Evolutionary consequences of changes in species' geographical
586   distributions driven by Milankovitch climate oscillations. *Proc. Natl. Acad. Sci. U. S. A.* **97**, 9115–9120
587   (2000).

588   44.   Devictor, V. *et al.* Spatial mismatch and congruence between taxonomic, phylogenetic and
589   functional diversity: the need for integrative conservation strategies in a changing world. *Ecol. Lett.*
590   **13**, no-no (2010).

591   45.   Pollock, L. J., Thuiller, W. & Jetz, W. Large conservation gains possible for global biodiversity facets.
592   *Nature* **546**, 141–144 (2017).

593   46.   Mazel, F., Mooers, A. O., Riva, G. V. D. & Pennell, M. W. Conserving Phylogenetic Diversity Can Be a
594   Poor Strategy for Conserving Functional Diversity. *Syst. Biol.* **66**, 1019–1027 (2017).

595   47.   Guo, W.-Y. *et al.* Half of the world's tree biodiversity is unprotected and is increasingly threatened
596   by human activities. *bioRxiv* 2020.04.21.052464 (2020). doi:10.1101/2020.04.21.052464

597   48.   Brown, J. H., Gillooly, J. F., Allen, A. P., Savage, V. M. & West, G. B. Toward a metabolic theory of
598   ecology. in *Ecology* **85**, 1771–1789 (2004).

599   49.   Brown, J. H. Why are there so many species in the tropics? *J. Biogeogr.* **41**, 8–22 (2014).

600   50.   Steinbauer, M. J. *et al.* Accelerated increase in plant species richness on mountain summits is linked
601   to warming. *Nature* **556**, 231–234 (2018).

602   51.   Gillooly, J. F. & Allen, A. P. Linking global patterns in biodiversity to evolutionary dynamics using
603   metabolic theory. *Ecology* **88**, 1890–4 (2007).

604   52.   Wright, I. J. *et al.* The worldwide leaf economics spectrum. *Nature* **428**, 821–827 (2004).

605   53.   Wright, I. J. *et al.* Global climatic drivers of leaf size. *Science (80-.).* **357**, 917–921 (2017).

606   54.   Swenson, N. G. *et al.* Constancy in functional space across a species richness anomaly. *Am. Nat.* **187**,
607   E83–E92 (2016).

608   55.   Ordonez, A. & Svenning, J. C. Greater tree species richness in eastern North America compared to
609   Europe is coupled to denser, more clustered functional trait space filling, not to trait space
610   expansion. *Glob. Ecol. Biogeogr.* **27**, 1288–1299 (2018).

611   56.   Beech, E., Rivers, M., Oldfield, S. & Smith, P. P. GlobalTreeSearch: The first complete global database
612   of tree species and country distributions. *J. Sustain. For.* **36**, 454–489 (2017).

613 57. Serra-Diaz, J. M., Enquist, B. J., Maitner, B., Merow, C. & Svenning, J. C. Big data of tree species
614   distributions: how big and how good? *For. Ecosyst.* **4**, 30 (2017).

615 58. Hillebrand, H. On the Generality of the Latitudinal Diversity Gradient. *Am. Nat.* **163**, 192–211 (2004).

616 59. Gaston, K. J. Global patterns in biodiversity. *Nature* **405**, 220–227 (2000).

617 60. Pianka, E. R. Latitudinal Gradients in Species Diversity: A Review of Concepts. *Am. Nat.* **100**, 33–46
618   (2002).

619 61. Barthlott, W. *et al.* Geographic Patterns of Vascular Plant Diversity at Continental to Global Scales
620   (Geographische Muster der Gefäßpflanzenvielfalt im kontinentalen und globalen Maßstab).
621   *Erdkunde* **61**, 305–315 (2007).

622 62. Lamanna, C. *et al.* Functional trait space and the latitudinal diversity gradient. *Proc. Natl. Acad. Sci. U.*
623   *S. A.* **111**, 13745–13750 (2014).

624 63. Wing, S. L. *et al.* Late Paleocene fossils from the Cerrejon Formation, Colombia, are the earliest
625   record of Neotropical rainforest. *Proc. Natl. Acad. Sci.* **106**, 18627–18632 (2009).

626 64. Antonelli, A. *et al.* Amazonia is the primary source of Neotropical biodiversity. *Proc. Natl. Acad. Sci.*
627   **115**, 6034–6039 (2018).

628 65. Chu, C. *et al.* Direct and indirect effects of climate on richness drive the latitudinal diversity gradient
629   in forest trees. *Ecology Letters* **22**, 245–255 (2019).

630 66. Fine, P. V. A. Ecological and Evolutionary Drivers of Geographic Variation in Species Diversity. *Annu.*
631   *Rev. Ecol. Evol. Syst.* **46**, 369–392 (2015).

632 67. Feng, G. *et al.* Species and phylogenetic endemism in angiosperm trees across the Northern
633   Hemisphere are jointly shaped by modern climate and glacial–interglacial climate change. *Glob. Ecol.*
634   *Biogeogr.* **28**, 1393–1402 (2019).

635 68. Kissling, W. D. *et al.* Quaternary and pre-Quaternary historical legacies in the global distribution of a
636   major tropical plant lineage. *Glob. Ecol. Biogeogr.* **21**, 909–921 (2012).

637 69. Blonder, B. *et al.* Linking environmental filtering and disequilibrium to biogeography with a
638   community climate framework. *Ecology* **96**, 972–985 (2015).

639 70. Ordonez, A. & Svenning, J. C. Functional diversity of North American broad-leaved trees is
640   codetermined by past and current environmental factors. *Ecosphere* **7**, (2016).

641 71. Pound, M. J., Haywood, A. M., Salzmann, U. & Riding, J. B. Global vegetation dynamics and
642   latitudinal temperature gradients during the Mid to Late Miocene (15.97–5.33Ma). *Earth-Science*
643   *Rev.* **112**, 1–22 (2012).

644 72. Osborne, C. P. Atmosphere, ecology and evolution: What drove the Miocene expansion of C4
645   grasslands? *Journal of Ecology* **96**, 35–45 (2008).

646 73. Greenop, R., Foster, G. L., Wilson, P. A. & Lear, C. H. Middle Miocene climate instability associated
647   with high-amplitude CO_2 variability. *Paleoceanography* **29**, 845–853 (2014).

648 74. Steinthorsdottir, M., Jardine, P. E. & Rember, W. C. Near-Future p CO_2 during the hot Mid Miocene
649   Climatic Optimum. *Paleoceanogr. Paleoclimatology* (2020). doi:10.1029/2020PA003900

650 75. Lucas, E. J. & Bünger, M. O. Myrtaceae in the Atlantic forest: their role as a 'model' group. *Biodivers.*
651   *Conserv.* **24**, 2165–2180 (2015).

652 76.   Deng, M., Jiang, X. L., Hipp, A. L., Manos, P. S. & Hahn, M. Phylogeny and biogeography of East Asian
653   evergreen oaks (Quercus section Cyclobalanopsis; Fagaceae): Insights into the Cenozoic history of
654   evergreen broad-leaved forests in subtropical Asia. *Mol. Phylogenet. Evol.* **119**, 170–181 (2018).

655 77.   Piñeiro, R., Dauby, G., Kaymak, E. & Hardy, O. J. Pleistocene population expansions of shade-tolerant
656   trees indicate fragmentation of the African rainforest during the ice ages. *Proc. R. Soc. B Biol. Sci.*
657   **284**, 20171800 (2017).

658 78.   Zozomová-Lihová, J., Melichárková, A., Svitok, M. & Španiel, S. Pleistocene range disruption and
659   postglacial expansion with secondary contacts explain the genetic and cytotype structure in the
660   western Balkan endemic Alyssum austrodalmaticum (Brassicaceae). *Plant Syst. Evol.* **306**, 1–25
661   (2020).

662 79.   Niinemets, Ü. & Valladares, F. Tolerance to shade, drought, and waterlogging of temperate northern
663   hemisphere trees and shrubs. *Ecol. Monogr.* **76**, 521–547 (2006).

664 80.   Conradi, T., Van Meerbeek, K., Ordonez, A. & Svenning, J. Biogeographic historical legacies in the net
665   primary productivity of Northern Hemisphere forests. *Ecol. Lett.* **23**, 800–810 (2020).

666 81.   Muscarella, R. *et al.* Functional convergence and phylogenetic divergence during secondary
667   succession of subtropical wet forests in Puerto Rico. *J. Veg. Sci.* **27**, 283–294 (2016).

668 82.   Swenson, N. G. & Enquist, B. J. Opposing assembly mechanisms in a Neotropical dry forest:
669   implications for phylogenetic and functional community ecology. *Ecology* **90**, 2161–2170 (2009).

670 83.   Kraft, N. J. B., Valencia, R. & Ackerly, D. D. Functional traits and niche-based tree community
671   assembly in an Amazonian forest. *Science (80-.).* **322**, 580–582 (2008).

672 84.   Hubbell, S. P. Neutral theory and the evolution of ecological equivalence. *Ecology* **87**, 1387–1398
673   (2006).

674 85.   Boyle, B. *et al.* The taxonomic name resolution service: An online tool for automated standardization
675   of plant names. *BMC Bioinformatics* **14**, 16 (2013).

676 86.   Enquist, B. J., Condit, R. R., Peet, R. K., Schildhauer, M. & Thiers, B. M. The Botanical Information and
677   Ecology Network (BIEN): Cyberinfrastructure for an integrated botanical information network to
678   investigate the ecological impacts of global climate change on plant biodiversity. *PeerJ* **4**, e2615v2
679   (2016).

680 87.   Enquist, B. J. *et al.* The commonness of rarity: Global and future distribution of rarity across land
681   plants. *Sci. Adv.* **5**, eaaz0414 (2019).

682 88.   Banda, K. R. *et al.* Plant diversity patterns in neotropical dry forests and their conservation
683   implications. *Science (80-.).* **353**, 1383–1387 (2016).

684 89.   Dauby, G. *et al.* RAINBIO: a mega-database of tropical African vascular plants distributions.
685   *PhytoKeys* **74**, 1–18 (2016).

686 90.   Pateiro-López, B. & Rodríguez-Casal, A. Generalizing the Convex Hull of a Sample: The R Package
687   alphahull. *J. Stat. Softw.* **34**, (2015).

688 91.   Kirkpatrick, D. G. & Seidel, R. On the Shape of a Set of Points in the Plane. *IEEE Trans. Inf. Theory* **29**,
689   551–559 (1983).

690 92.   R Core Team. R: A Language and Environment for Statistical Computing. (2019).

93.   Vilela, B. & Villalobos, F. LetsR: A new R package for data handling and analysis in macroecology. *Methods Ecol. Evol.* **6**, 1229–1234 (2015).

94.   Smith, S. A. & Brown, J. W. Constructing a broadly inclusive seed plant phylogeny. *Am. J. Bot.* **105**, 302–314 (2018).

95.   Magallón, S., Gómez-Acevedo, S., Sánchez-Reyes, L. L. & Hernández-Hernández, T. A metacalibrated time-tree documents the early rise of flowering plant phylogenetic diversity. *New Phytol.* **207**, 437–453 (2015).

96.   Díaz, S. *et al.* The global spectrum of plant form and function. *Nature* **529**, 167–171 (2016).

97.   Kattge, J. *et al.* TRY - a global database of plant traits. *Glob. Chang. Biol.* **17**, 2905–2935 (2011).

98.   Kattge, J. *et al.* TRY plant trait database – enhanced coverage and open access. *Glob. Chang. Biol.* **26**, 119–188 (2020).

99.   Aubin, I., Beaudet, M. & Messier, C. Light extinction coefficients specific to the understory vegetation of the southern boreal forest, Quebec. *Can. J. For. Res.* **30**, 168–177 (2000).

100. Aubin, I., Messier, C. & Kneeshaw, D. Population structure and growth acclimation of mountain maple along a successional gradient in the southern boreal forest. *Écoscience* **12**, 540–548 (2005).

101. Aubin, I. *et al.* Traits to stay, traits to move: A review of functional traits to assess sensitivity and adaptive capacity of temperate and boreal trees to climate change. *Environmental Reviews* **24**, 164–186 (2016).

102. Thiffault, N., Titus, B. D. & Munson, A. D. Silvicultural options to promote seedling establishment on Kalmia-Vaccinium-dominated sites. *Scand. J. For. Res.* **20**, 110–121 (2005).

103. Titus, B. D. *et al.* Post-harvest nitrogen cycling in clearcut and alternative silvicultural systems in a montane forest in coastal British Columbia. *For. Chron.* **82**, 844–859 (2006).

104. Wiebe, S., Morris, D., Luckai, N. & Reid, D. Coarse Woody Debris Dynamics Following Biomass Harvesting: Tracking Carbon and Nitrogen Patterns During Early Stand Development in Upland Black Spruce Ecosystems. *Int. J. For. Eng.* **23**, 25–32 (2012).

105. Masse, J., Prescott, C. E., Müller, C. & Grayston, S. J. Gross nitrogen transformation rates differ in reconstructed oil-sand soils from natural boreal-forest soils as revealed using a 15N tracing method. *Geoderma* **282**, 37–48 (2016).

106. Shan, H. *et al.* Gap Filling in the Plant Kingdom---Trait Prediction Using Hierarchical Probabilistic Matrix Factorization. in *Proceedings of the 29th International Conference on Machine Learning* 1303–1310 (2012).

107. Fazayeli, F., Banerjee, A., Kattge, J., Schrodt, F. & Reich, P. B. Uncertainty quantified matrix completion using bayesian hierarchical matrix factorization. in *Proceedings - 2014 13th International Conference on Machine Learning and Applications, ICMLA 2014* 312–317 (IEEE, 2014). doi:10.1109/ICMLA.2014.56

108. Schrodt, F. *et al.* BHPMF - a hierarchical Bayesian approach to gap-filling and trait prediction for macroecology and functional biogeography. *Glob. Ecol. Biogeogr.* **24**, 1510–1521 (2015).

109. Dynesius, M. & Jansson, R. Evolutionary consequences of changes in species' geographical distributions driven by Milankovitch climate oscillations. *Proc. Natl. Acad. Sci.* **97**, 9115–9120 (2000).

730   110.   Jetz, W. & Rahbek, C. Geographic range size and determinants of avian species richness. *Science (80-*
731   *.).* **297**, 1548–1551 (2002).

732   111.   Fick, S. E. & Hijmans, R. J. WorldClim 2: new 1-km spatial resolution climate surfaces for global land
733   areas. *Int. J. Climatol.* **37**, 4302–4315 (2017).

734   112.   Hill, D. J. The non-analogue nature of Pliocene temperature gradients. *Earth Planet. Sci. Lett.* **425**,
735   232–241 (2015).

736   113.   Brown, J. L., Hill, D. J., Dolan, A. M., Carnaval, A. C. & Haywood, A. M. Paleoclim, high spatial
737   resolution paleoclimate surfaces for global land areas. *Sci. Data* **5**, 180254 (2018).

738   114.   Dolan, A. M. *et al.* Modelling the enigmatic Late Pliocene Glacial Event - Marine Isotope Stage M2.
739   *Glob. Planet. Change* **128**, 47–60 (2015).

740   115.   Karger, D. N. *et al.* Climatologies at high resolution for the earth's land surface areas. *Sci. Data* **4**,
741   170122 (2017).

742   116.   Otto-Bliesner, B. L., Marshall, S. J., Overpeck, J. T., Miller, G. H. & Hu, A. Simulating arctic climate
743   warmth and icefield retreat in the last interglaciation. *Science (80-.).* **311**, 1751–1753 (2006).

744   117.   Kreft, H. & Jetz, W. Global patterns and determinants of vascular plant diversity. *Proc. Natl. Acad. Sci.*
745   **104**, 5925–5930 (2007).

746   118.   Zhang, J., Nielsen, S. E., Mao, L., Chen, S. & Svenning, J. C. Regional and historical factors supplement
747   current climate in shaping global forest canopy height. *J. Ecol.* **104**, 469–478 (2016).

748   119.   Kennedy, C. M., Oakleaf, J. R., Theobald, D. M., Baruch-Mordo, S. & Kiesecker, J. Managing the
749   middle: A shift in conservation priorities based on the global human modification gradient. *Glob.*
750   *Chang. Biol.* **25**, 811–826 (2019).

751   120.   Sanderson, E. W. *et al.* The Human Footprint and the Last of the Wild. *Bioscience* **52**, 891–904 (2002).

752   121.   Schulze, K. *et al.* An assessment of threats to terrestrial protected areas. *Conservation Letters* **11**,
753   e12435 (2018).

754   122.   Slavich, E., Warton, D. I., Ashcroft, M. B., Gollan, J. R. & Ramp, D. Topoclimate versus macroclimate:
755   How does climate mapping methodology affect species distribution models and climate change
756   projections? *Divers. Distrib.* **20**, 952–963 (2014).

757   123.   Stein, A., Gerstner, K. & Kreft, H. Environmental heterogeneity as a universal driver of species
758   richness across taxa, biomes and spatial scales. *Ecology Letters* **17**, 866–880 (2014).

759   124.   Morrone, J. J. Biogeographical regions under track and cladistic scrutiny. *Journal of Biogeography* **29**,
760   149–152 (2002).

761   125.   Olson, D. M. *et al.* Terrestrial Ecoregions of the World: A New Map of Life on Earth. *Bioscience* **51**,
762   933 (2001).

763   126.   Harter, D. E. V. *et al.* Impacts of global climate change on the floras of oceanic islands - Projections,
764   implications and current knowledge. *Perspectives in Plant Ecology, Evolution and Systematics* **17**,
765   160–183 (2015).

766   127.   Mouchet, M. *et al.* Towards a consensus for calculating dendrogram-based functional diversity
767   indices. *Oikos* **117**, 794–800 (2008).

768   128.   Oksanen, J. *et al.* vegan: Community Ecology Package. (2019).

769   129.   Müllner, D. fastcluster⬚: Fast Hierarchical, Agglomerative Clustering Routines for R and Python. *J.*
770   *Stat. Softw.* **53**, 1–18 (2015).

771   130.   Kembel, S. W. *et al.* Picante: R tools for integrating phylogenies and ecology. *Bioinformatics* **26**,
772   1463–1464 (2010).

773   131.   Osorio, F., Vallejos, R. & Cuevas, F. SpatialPack: Computing the Association Between Two Spatial
774   Processes. (2016).

775   132.   Kissling, W. D. & Carl, G. Spatial autocorrelation and the selection of simultaneous autoregressive
776   models. *Glob. Ecol. Biogeogr.* **17**, 59–71 (2008).

777   133.   Nagelkerke, N. J. D. A note on a general definition of the coefficient of determination. *Biometrika* **78**,
778   691–692 (1991).

779   134.   Burnham, K. P. & Anderson, D. R. Multimodel inference: Understanding AIC and BIC in model
780   selection. *Sociological Methods and Research* **33**, 261–304 (2004).

781   135.   Bivand, R. S. & Wong, D. W. S. Comparing implementations of global and local indicators of spatial
782   association. *Test* **27**, 716–748 (2018).

783   136.   Schielzeth, H. Simple means to improve the interpretability of regression coefficients. *Methods Ecol.*
784   *Evol.* **1**, 103–113 (2010).

Acknowledgments

We thank Brad Boyle for valuable database and informatics assistance and advice, and TRY contributors for sharing their data. This work was conducted as a part of the BIEN Working Group, 2008–2012. We thank all the data contributors and numerous herbaria who have contributed their data to various data compiling organizations (see the herbarium list below) for the invaluable data and support provided to BIEN. We thank the New York Botanical Garden; Missouri Botanical Garden; Utrecht Herbarium; the UNC Herbarium; and GBIF, REMIB, and SpeciesLink. The staff at CyVerse provided critical computational assistance.

We acknowledge the herbaria that contributed data to this work: A, AAH, AAS, AAU, ABH, ACAD, ACOR, AD, AFS, AK, AKPM, ALCB, ALTA, ALU, AMD, AMES, AMNH, AMO, ANGU, ANSM, ANSP, AQP, ARAN, ARIZ, AS, ASDM, ASU, AUT, AV, AWH, B, BA, BAA, BAB, BABY, BACP, BAF, BAFC, BAI, BAJ, BAL, BARC, BAS, BBB, BBS, BC, BCMEX, BCN, BCRU, BEREA, BESA, BG, BH, BHCB, BIO, BISH, BLA, BM, BOCH, BOL, BOLV, BONN, BOON, BOTU, BOUM, BPI, BR, BREM, BRI, BRIT, BRLU, BRM, BSB, BUT, C, CALI, CAN, CANB, CANU, CAS, CATA, CATIE, CAY, CBM, CDA, CDBI, CEN, CEPEC, CESJ, CGE, CGMS, CHAM, CHAPA, CHAS, CHR, CHSC, CIB, CICY, CIIDIR, CIMI, CINC, CLEMS, CLF, CMM, CMMEX, CNPO, CNS, COA, COAH, COCA, CODAGEM, COFC, COL, COLO, CONC, CORD, CP, CPAP, CPUN, CR, CRAI, CRP, CS, CSU, CSUSB, CTES, CTESN, CU, CUVC, CUZ, CVRD, DAO, DAV, DBG, DBN, DES, DLF, DNA, DPU, DR, DS, DSM, DUKE, DUSS, E, EA, EAC, EAN, EBUM, ECON, EIF, EIU, EMMA, ENCB, ER, ERA, ESA, ETH, F, FAA, FAU, FAUC, FB, FCME, FCO, FCQ, FEN, FHO, FI, FLAS, FLOR, FM, FR, FRU, FSU, FTG, FUEL, FULD, FURB, G, GAT, GB, GDA, GENT, GES, GH, GI, GLM, GMDRC, GMNHJ, GOET, GRA, GUA, GZU, H, HA, HAC, HAL, HAM, HAMAB, HAO, HAS, HASU, HB, HBG, HBR, HCIB, HEID, HGM, HIB, HIP, HNT, HO, HPL, HRCB, HRP, HSC, HSS, HU, HUA, HUAA, HUAL, HUAZ, HUCP, HUEFS, HUEM, HUFU, HUJ, HUSA, HUT, HXBH, HYO, IAA, IAC, IAN, IB, IBGE, IBK, IBSC, IBUG, ICEL, ICESI, ICN, IEA, IEB, ILL, ILLS, IMSSM, INB, INEGI, INIF, INM, INPA, IPA, IPRN, IRVC, ISC, ISKW, ISL, ISTC, ISU, IZAC, IZTA, JACA, JBAG, JBGP, JCT, JE, JEPS, JOTR, JROH, JUA, JYV, K, KIEL, KMN, KMNH, KOELN, KOR, KPM, KSC, KSTC, KSU, KTU, KU, KUN, KYO, L, LA, LAGU, LBG, LD, LE, LEB, LIL, LINC, LINN, LISE, LISI, LISU, LL, LMS, LOJA, LOMA, LP, LPAG, LPB, LPD, LPS, LSU, LSUM, LTB, LTR, LW, LYJB, LZ, M, MA, MACF, MAF, MAK, MARS, MARY, MASS, MB, MBK, MBM, MBML,

Author contributions

854   W.-Y.G., J.M.S.-D., and J.-C.S. conceived the project; J.M.S.-D., W.-Y.G., and all others collected

855   the data; W.-Y.G. analyzed the data; W.-Y.G. interpreted the data; W.-Y.G., J.M.S.-D., and J.-C.S.

856   wrote the manuscript. All authors contributed data, discussed the results, revised manuscript drafts,

857   and contributed to writing and approved the final manuscript.

Competing interests

859   The authors declare no competing interests.

Data and materials availability:

861   All the occurrences are deposited in BIEN (https://bien.nceas.ucsb.edu/bien/), and the phylogeny

862   and imputed functional trait data are available via ref. [47].
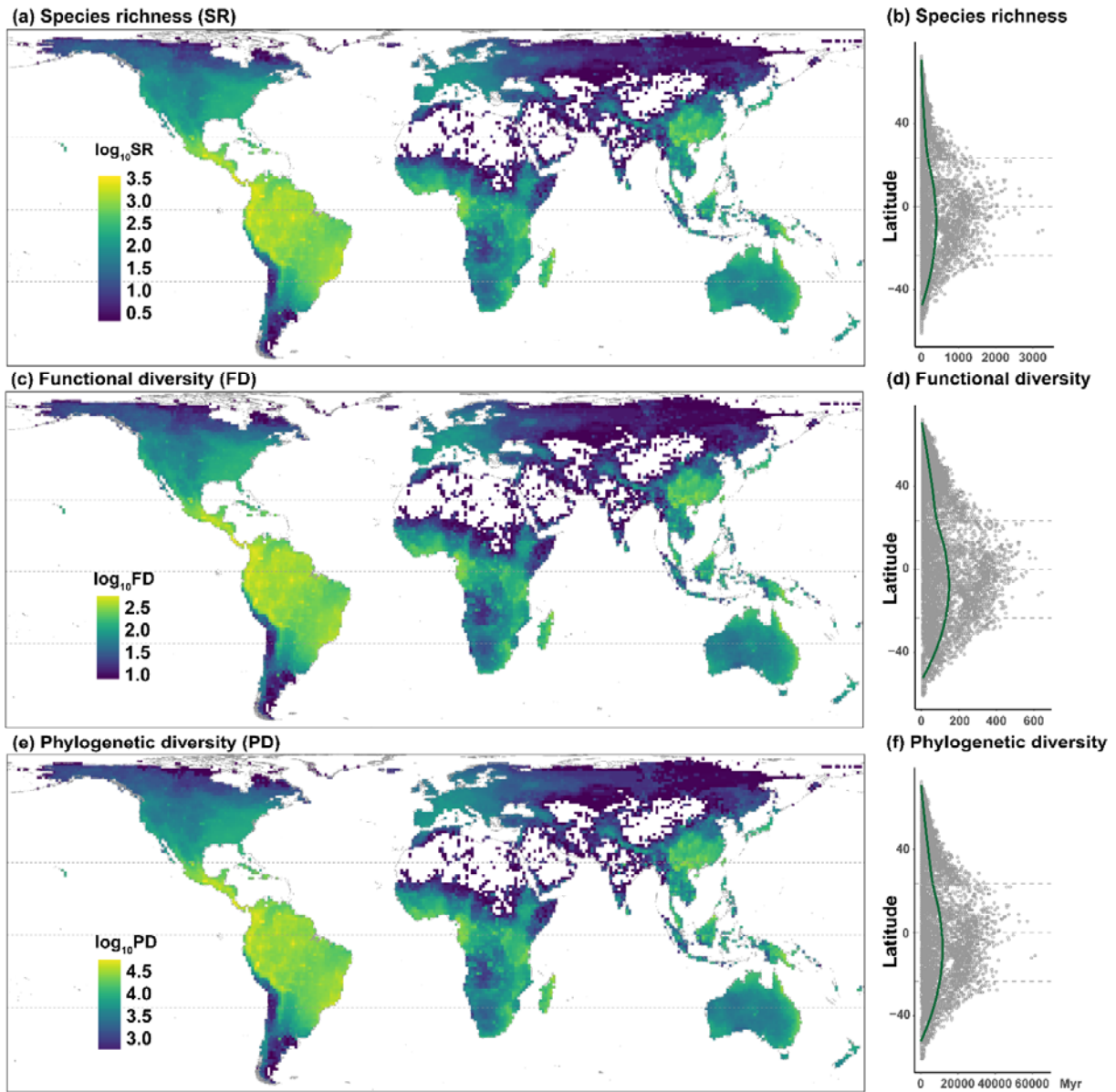
Figures

Fig. 1 Global patterns of tree (a) species richness, (c) functional diversity, and (e) phylogenetic diversity. In (b), (d) and (f), the fitted line is the lowess regression. Maps use the Behrmann projection at 110 km × 110 km spatial resolution. Myr: Million years.
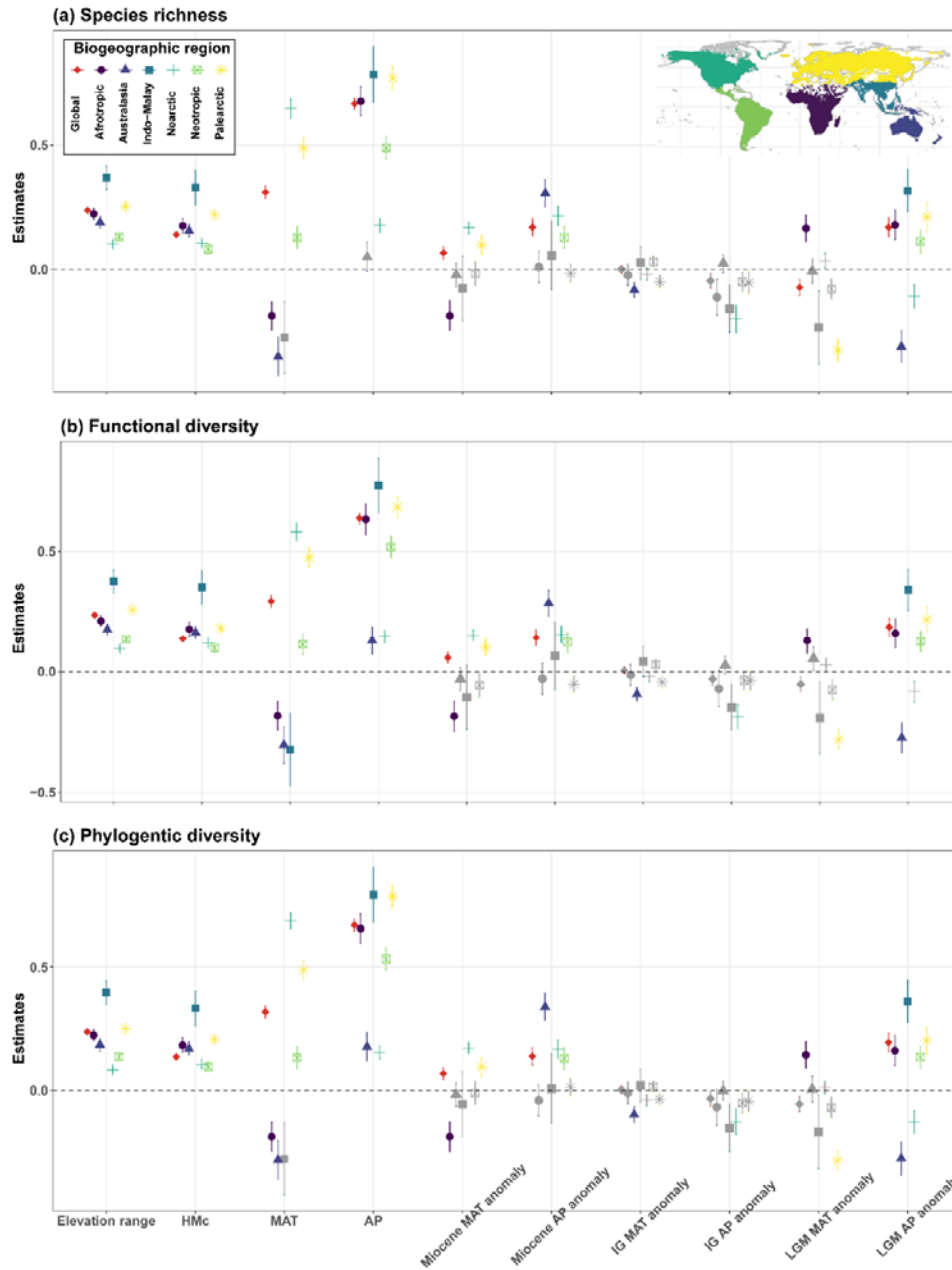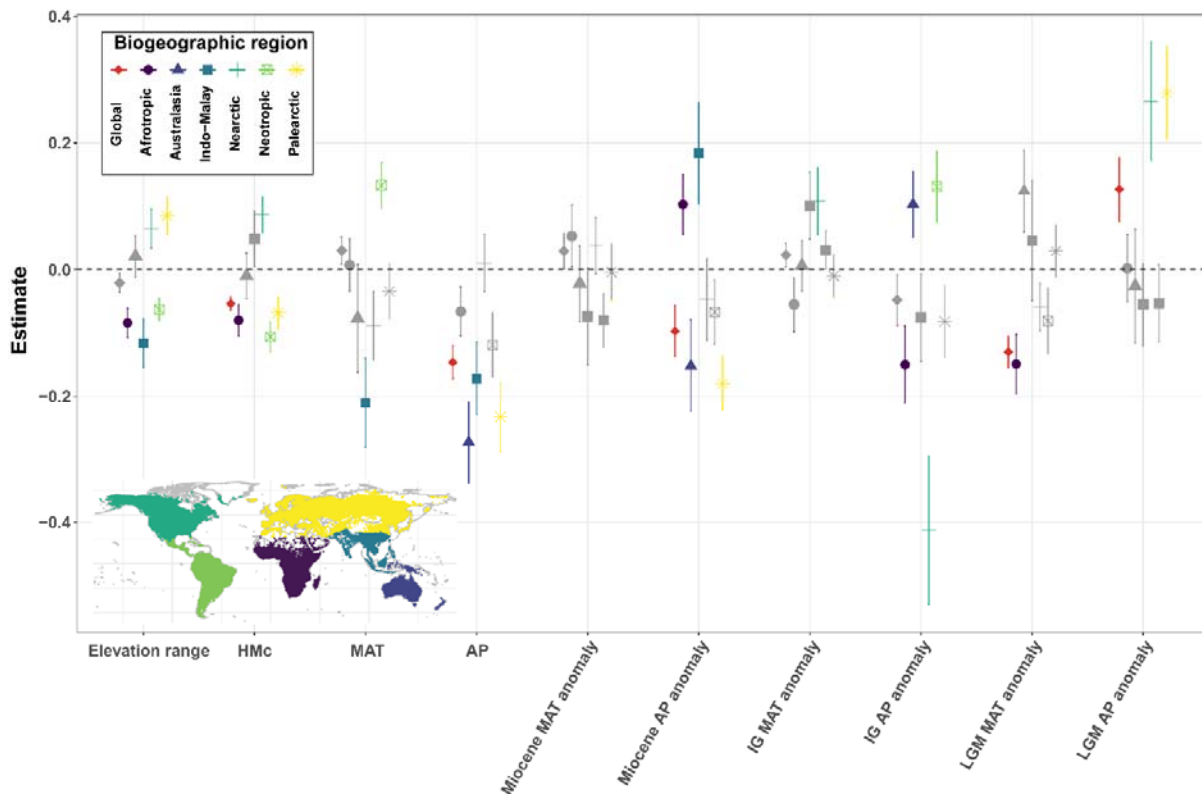
Fig. 2 Effects of the tested environmental variables on tree (a) specie richness (SR), (b) functional diversity

(FD) and (c) phylogenetic diversity (PD). Estimates (± 1standard error) of effects were obtained from

simultaneous autoregressive (SAR) models. Different colors and shapes indicate biogeographic regions.

Non-significant variables ($p > 0.05$) are indicated in grey. Results from OLS models are shown in Table S2.

HMc: human modification index; MAT: mean annual temperature; AP: Annual precipitation; IG: Pleistocene

Interglacial; LGM: Last Glacial Maximum. Anomaly was calculated as the past minus the present state.

874
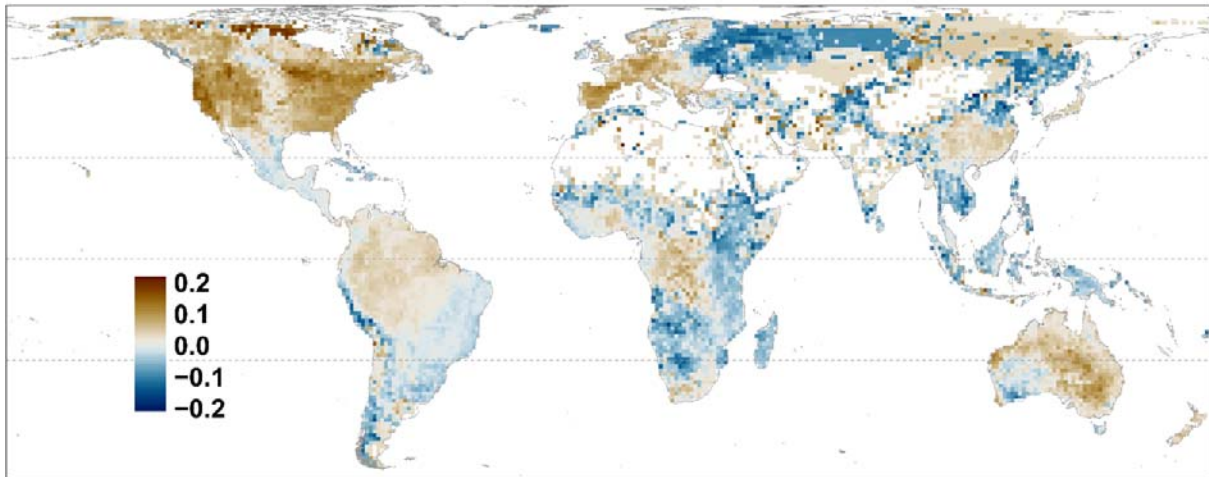
Fig. 3 Global patterns of the residuals (deviation) from the ordinary least regression between functional diversity (FD) and phylogenetic diversity (PD) (FD = 0.90PD, R^2 = 0.987, $p < 0.0001$). Brown (positive) areas are areas of higher FD than expected based on PD, whereas blue (negative) areas depict areas with lower FD than expected from the observed PD. Map uses the Behrmann projection at 110 km × 110 km spatial resolution.

880

Fig. 4 Effects of the tested environmental variables on the residuals from the regression between functional

diversity (FD) and phylogenetic diversity (PD) (Fig. 3). Estimate (± 1standard error) of effects were obtained

from simultaneous autoregressive (SAR) models. Different colors and shapes indicate biogeographic regions.

Non-significant variables ($p > 0.05$) are indicated in grey. Results from OLS models are shown in Table S3.

HMc: human modification index; MAT: mean annual temperature; AP: Annual precipitation; IG: Pleistocene

Interglacial; LGM: Last Glacial Maximum. Anomaly was calculated as the past minus the present state.
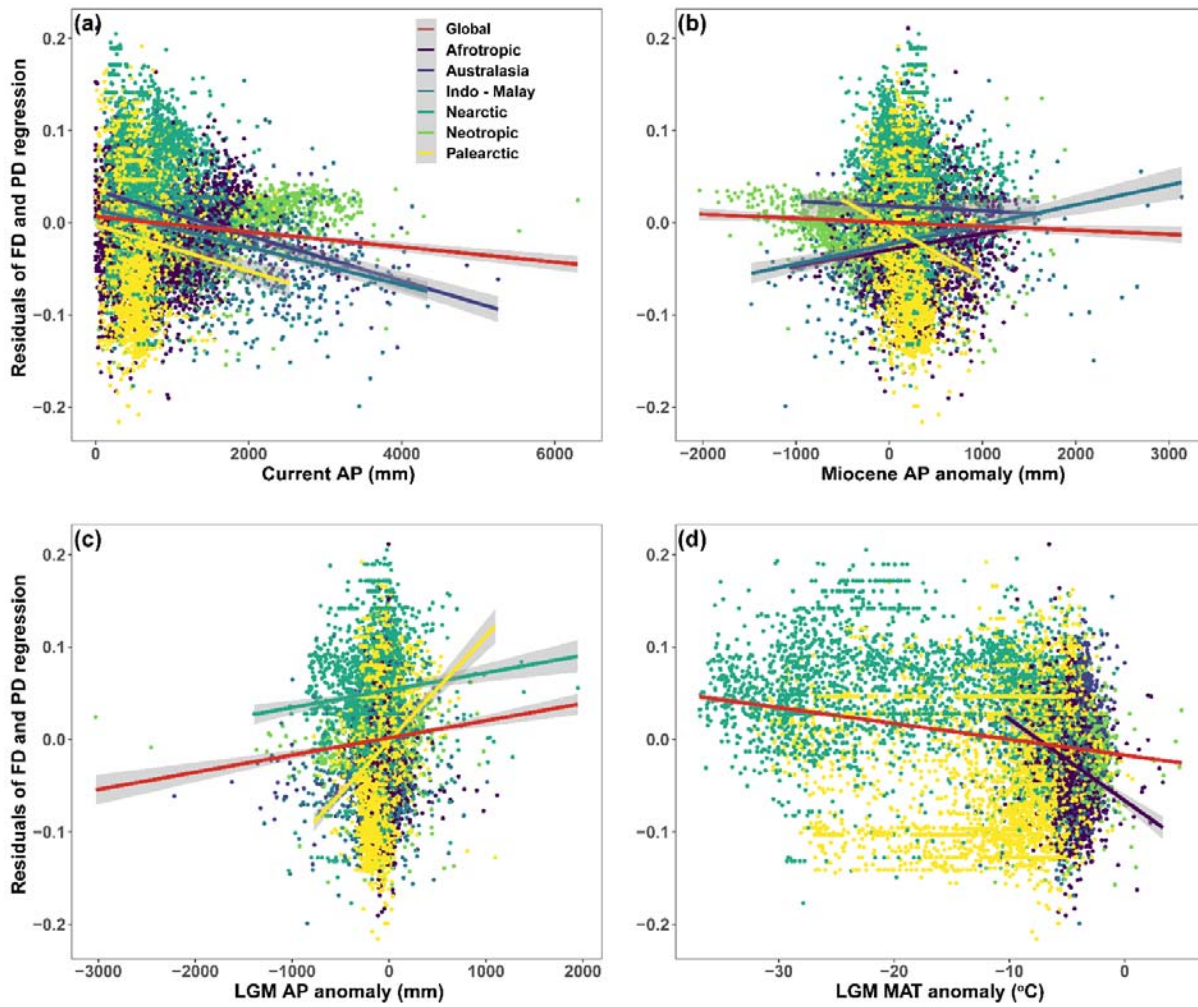
Fig. 5 Bivariate regressions between the residuals from the regression of functional diversity (FD) on

phylogenetic diversity (PD) and significant explanatory climate variables. Anomaly was calculated as the

past minus the present state. For each subplot, only significant relationships are shown (Fig. 4, $p < 0.05$).